Volume 5 | Number 29 | 7 August 2017 | Pages 7113–7362

Journal of Materials Chemistry C

Materials for optical, magnetic and electronic devices

rsc.li/materials-c

ISSN 2050-7526

ROYAL SOCIETY OF CHEMISTRY

PAPER

Chong-Xin Shan, Lin Dong, De-Zhen Shen *et al.*

Advanced encryption based on fluorescence quenching of ZnO nanoparticles

Journal of Materials Chemistry C

PAPER

View Article Online
View Journal | View Issue

Cite this: J. Mater. Chem. C, 2017, 5, 7167

Advanced encryption based on fluorescence quenching of ZnO nanoparticles†

Kai-Kai Liu,[ab] Chong-Xin Shan,*[ac] Gao-Hang He,[ab] Ruo-Qiu Wang,[a] Zhi-Peng Sun,[ab] Quan Liu,[ab] Lin Dong*[c] and De-Zhen Shen*[a]

Received 15th May 2017,
Accepted 8th June 2017

DOI: 10.1039/c7tc02095c

rsc.li/materials-c

Encryption is of vital importance in both military and civil fields. Although there have been a few attempts to encrypt information and produce anti-counterfeiting techniques employing functional materials, it is still urgently needed to develop advanced encryption routes that cannot be cracked easily. This paper presents a simple strategy for advanced encryption based on the fluorescence quenching of ZnO nanoparticles (NPs) by acid and copper ions. In this strategy, certain patterns are printed onto a ZnO NP pre-coated paper using a $CuCl_2$ aqueous solution as an ink to produce an invisible latent image, which is only visible under ultraviolet (UV) irradiation. For encryption, the patterns can be perfectly concealed by exposure to vinegar vapour, due to the dissolution of the ZnO NPs in acidic conditions, and decryption can be performed *via* neutralization in an ambient soda vapour environment and subsequent uniform re-coating with ZnO NPs. An additional matrix of pixels with encoded grey levels acquired by tuning the dose of $CuCl_2$ is demonstrated to further enhance the anti-counterfeiting capability. A 4 × 4 micron matrix with a total combination of 1.67×10^8 codes has been enciphered in the latent patterns for demonstration, and this is a huge barrier for counterfeiting. The results reported in this paper provide a simple strategy for advanced encryption, and may inspire versatile applications in the fields of information security and anti-counterfeiting.

1 Introduction

Information security is vitally important for applications in some specific fields, for example economic activities, social activities, and individual and military communications. In recent years, a wide variety of functional materials[1–9] that are responsive to external stimuli have been investigated for data recording and storage,[10–13] among which fluorescent NPs have been widely regarded as one of the most promising candidates for security printing. Quite a few attempts of data recording and storage,[14,15] anti-counterfeiting,[16–21] and information encryption[22–27] using fluorescent NPs have been reported. Typically, certain patterns for encryption are written or printed using the fluorescent NPs as an ink, which is invisible under normal conditions but visible under certain illumination or chemical conditions.[28–30] Although the above technology can be applied in encryption,[31–33] it is easy to be cracked.[34] An alternative route for encryption is to employ external stimuli as "pens" to produce patterns on functionally coated "security paper", and using fluorescence lifetime imaging microscopy to differentiate the patterns from the background.[35] However, the above processes are extraordinarily complex for users and thus their future applications for information encryption are drastically hindered. It is urgently needed to develop advanced information encryption techniques that can be easily carried out but cannot be cracked easily.

ZnO NPs, as one of the eco-friendly semiconductor NPs, have been reported to be widely used in cell imaging and biosensing,[36,37] drug delivery,[38–40] photodetectors[41–43] and photoconductors,[44] electron transport layers[45–47] and dielectric layers,[48] *etc.* However, no previous reports have been found in the information security field using ZnO NPs. Although ZnO has been criticized for its chemical instability,[49,50] this instability can be fully leveraged to improve information safety. Here, a simple strategy for advanced encryption is demonstrated by employing ZnO NPs as the fluorescent agent and $CuCl_2$ and vinegar as the ink and quencher, respectively. Under UV illumination, bright yellowish fluorescence will be observed from the NPs, which can be quenched by either $CuCl_2$[51–53] or acid.[36] Fluorescence quenched by vinegar can be recovered after a neutralizing process using soda followed by re-coating with ZnO NPs, while the $CuCl_2$ quenched fluorescence cannot be recovered. On the

[a] State Key Laboratory of Luminescence and Applications, Changchun Institute of Optics, Fine Mechanics and Physics, Chinese Academy of Sciences, Changchun 130033, China. E-mail: shancx@ciomp.ac.cn
[b] University of Chinese Academy of Sciences, Beijing 100049, China
[c] School of Physics and Engineering, Zhengzhou University, Zhengzhou 450001, China

† Electronic supplementary information (ESI) available. See DOI: 10.1039/c7tc02095c

basis of such distinct quenching phenomena, $CuCl_2$ and vinegar can be used as the ink and quencher to generate and conceal the patterns to be enciphered, respectively, on ZnO NP coated paper. Furthermore, the encrypted patterns can be further encoded using a matrix with a variety of grey levels produced by modulating the dose of the $CuCl_2$ solution for advanced information encryption and anti-counterfeiting.

2 Experimental sections

2.1 Materials

Zinc acetate dihydrate ($Zn(Ac)_2{\cdot}2H_2O$, purity 99%), potassium hydroxide (KOH, purity 95%), 3-aminopropyltriethoxysilane (APTES, purity 98%) and ethanol (purity 99.9%) were all of analytical grade and were purchased from Aladdin. Vinegar and sodium carbonate (soda) (edible grade, Shanxi Mature Vinegar Group Co., Ltd and Hubei Shuanghuan Science and Technology Stock Co., Ltd) were purchased from a supermarket. The vinegar, soda, and all other chemical reagents were used as received without further purification.

2.2 Synthesis of ZnO NPs

Water-soluble ZnO NPs were prepared using a two-step precipitation method. For a typical synthesis, at the first step 5.5 g $Zn(Ac)_2{\cdot}2H_2O$ was put into a beaker with a 150 mL ethanol solution, and then the solution was stirred with a 20 mL 1.75 M KOH ethanol solution under room temperature for 5 minutes, resulting in a transparent and colorless solution of ZnO NPs. The second step was performed by adding a mixed solution of 400 μL APTES and 2 mL deionized water dropwise. After this, APTES underwent hydrolysis under the water conditions and interacted with the ZnO NPs to form silane surface modified ZnO NPs. Finally, the precipitate was centrifuged by a centrifuge (6000 rpm, 2 minutes) and the precipitate was washed twice with ethanol to remove the unreacted precursors. The washed precipitate was dissolved into water for further applications.

2.3 Characterizations

The structural properties of the ZnO NPs were characterized using a JEM-2010 transmission electron microscope (TEM). The composition and bonding state of the ZnO NPs were measured using a Thermo ESCALAB-250 X-ray photoelectron spectrometer (XPS). The radicals in the ZnO NPs have been characterized using a Bruker VERTEX-70 Fourier transform infrared (FTIR) spectrometer. The fluorescence properties of the NPs were evaluated in a Hitachi F-7000 spectrophotometer employing the 365 nm line of a xenon lamp as the excitation source. The absorption spectra of the samples were acquired on a Shimadzu UV-3101PC spectrometer. The transient photoluminescence of the ZnO NPs was recorded on a FLS-920 fluorescence spectrometer.

3 Results and discussion

3.1 Structural characterization and optical properties of the ZnO NPs

The synthesis process of water-soluble ZnO NPs has been modified based on our previous work from a practical perspective.[54] Note that, all of the process can be performed at room temperature, and the time of the process is less than 10 min, as shown in Scheme 1. A drop of 0.5 mol L^{-1} ZnO NPs was dropped onto the surface of the copper grid, and then dried for 3 hours for observation with a transmission electron microscope (TEM). The morphology and structural characterization of the ZnO NPs employed as the fluorescent reagent for the encryption are shown in Fig. 1(a). The NPs are spherical in shape with a diameter ranging from 3–5 nm, and clear lattice fringes with a spacing of about 0.26 nm can be observed, as indicated in the inset of Fig. 1(a). Note that the NPs that have been modified by APTES are based on ethanol-soluble NPs. Energy dispersive X-ray spectroscopy (EDS) has been used to evaluate the composition of the NPs (see Fig. S1, ESI†); the diffraction peaks from the X-ray diffraction (XRD) pattern of the NPs are attributed to the diffraction of wurtzite ZnO (Fig. S2, ESI†). The FTIR and XPS spectra of the NPs indicate that silane has been coated onto the ZnO NPs (Fig. S3 and S4, ESI†).[55]

The excitation spectrum, fluorescence images, and spectra of the ZnO NP aqueous solution under UV irradiation are shown in Fig. 1(b). The photoluminescence excitation spectrum (PLE) marked with a dashed line is centred at around 365 nm, and the inset illustrates the emission image of the NP solution under the illumination of a 365 nm mercury lamp. Yellowish fluorescence can be observed from the solution, and the fluorescence spectra of the NPs are dominated by a broad emission peak at around 525 nm, which can be attributed to the deep-level emission of ZnO.[56–58] The fluorescence intensity of the NPs increases with their concentration in the investigated range from 0.06 to 0.5 mol L^{-1}. The size distribution of the ZnO NPs (0.5 mol L^{-1}) has been measured using the dynamic light scattering analysis (DLS) method, which was used to analyse the aggregation of ZnO NPs (Fig. S5, ESI†).

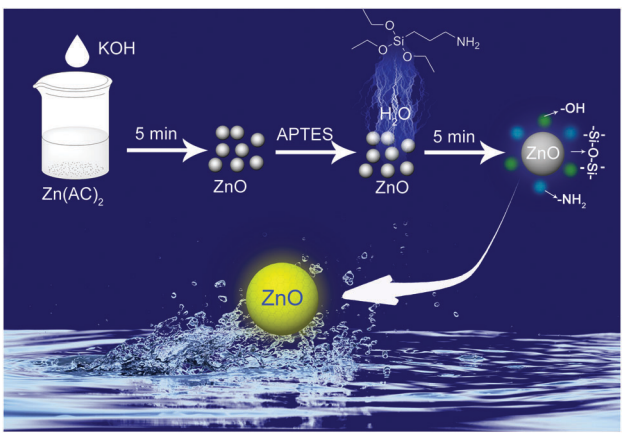

Scheme 1 Schematics of the preparation of water-soluble ZnO NPs.

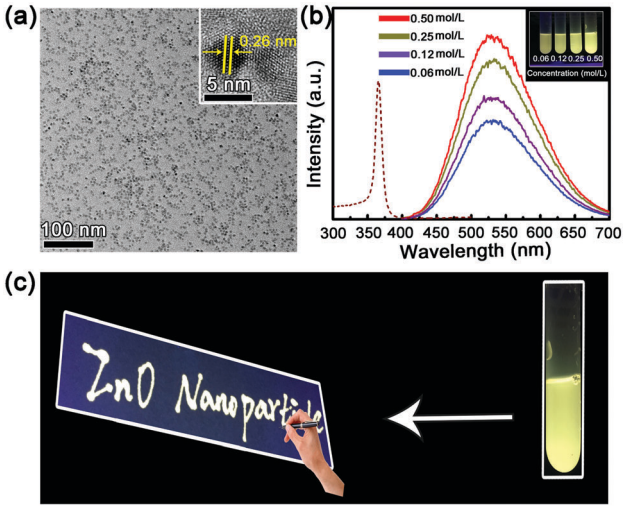

Fig. 1 (a) A TEM image of the ZnO NPs, with a high resolution TEM image of the NPs (inset). (b) Fluorescence spectra of the NPs with concentrations ranging from 0.06 mol L^{-1} to 0.5 mol L^{-1} under UV illumination; the excitation spectrum is marked by a dashed line and the inset shows the fluorescence image. (c) The words "ZnO Nanoparticle" written using the ZnO NP solution as ink on fluorescer-free paper.

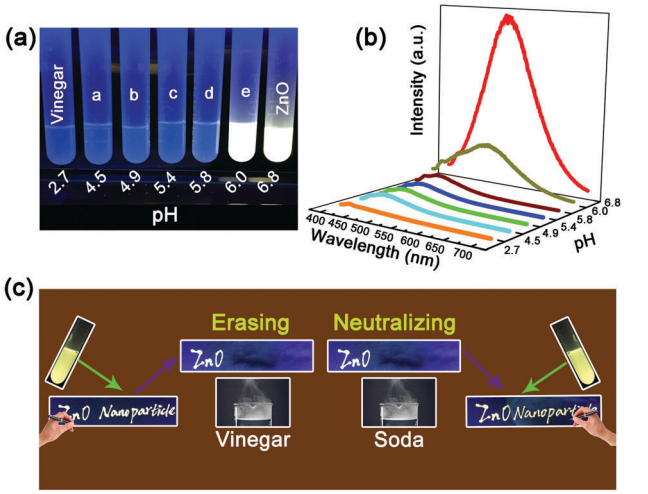

Fig. 2 (a) The fluorescence images of the NPs at different pH values. (b) The fluorescence spectra of the NPs at different pH values. (c) The words "ZnO Nanoparticle" written using the NPs as ink, and then the words were erased using vinegar vapour and rewritten when the adsorbed vinegar was neutralized using soda vapour.

The size of the ZnO NPs shows a narrow distribution with the center at around 6 nm, which is roughly consistent with the TEM observations shown in Fig. S5(a) (ESI†) (3–5 nm). Using the ZnO NPs with a concentration of 0.5 mol L^{-1} as fluorescent ink, several words have been written on fluorescer-free paper. Under normal indoor lighting conditions, the words are invisible; while they can be observed clearly under the illumination of the 365 nm line of a mercury lamp, as indicated in Fig. 1(c). The appearance of the written words under UV illumination results from the fluorescent nature of the ZnO NPs. The above results indicate that the fluorescence of the ZnO NPs can still be observed when the NPs are coated onto paper, which lays a solid ground for the encryption process described later.

3.2 Fluorescence quenching of the ZnO NPs

It is found that the fluorescence of the ZnO NPs is highly sensitive to the pH value of the ambient environment, as indicated in Fig. 2(a) and (b). The fluorescence spectrum of the vinegar incorporated ZnO NP solution consists of two emission bands, one at around 525 nm, and the other at around 450 nm. The former comes from the deep-level emission of ZnO, while the latter is from the fluorescence of the vinegar. Note that the fluorescence at around the 525 nm band is almost undetectable when the pH value of the solution is lower than 5.8, while the band at around 450 nm remains (Fig. S6, ESI†). The above fluorescence quenching is primarily caused by the decomposition of the NPs in an acidic environment.[59] The disappearance of the emission at around 525 nm reveals that the ZnO NPs have been decomposed almost completely when the pH value of the solution is lower than 5.8. The significant quenching of the fluorescence indicates that the words written using the ZnO NPs can be erased effectively by acidic reagents, such as vinegar.

It is also expected that when the surrounding environment of the ZnO NPs is neutralized words can be rewritten onto the paper again, and the schematic illustration of the above process is shown in Fig. 2(c).

The fluorescence of the ZnO NPs can also be quenched by copper ions, as indicated in Fig. 3. To study the quenching effect, a copper chloride ($CuCl_2$) aqueous solution was added into the ZnO NP solution, and the fluorescence spectra and images of the mixed solution are shown in Fig. 3(a). With increasing the amount of $CuCl_2$, the line-shape and emission position of the ZnO NPs remain almost unchanged, but the intensity decreases gradually. To explore the fluorescence quenching mechanism of the ZnO NPs by $CuCl_2$, the absorption

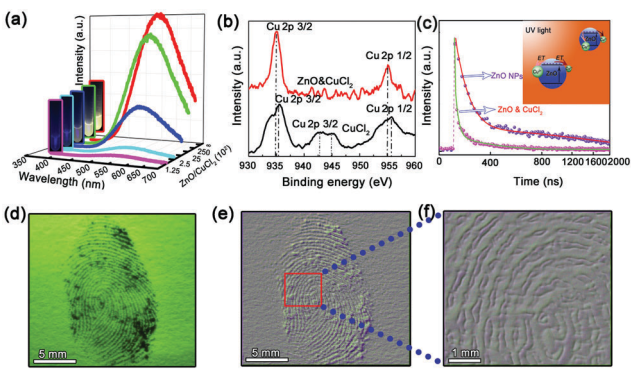

Fig. 3 (a) The fluorescence images and spectra of the ZnO NP solution with different $CuCl_2$ concentrations. (b) The Cu 2p XPS patterns of the $CuCl_2$ and ZnO NP/$CuCl_2$ mixed sample. (c) Transient spectra of the emission at around 525 nm for ZnO NPs and ZnO NP/$CuCl_2$ mixed sample. The inset shows the schematic illustration of electron transfer from the ZnO NPs to the $CuCl_2$. (d) A photograph of a fingerprint after pressing a finger dipped into the $CuCl_2$ solution onto the ZnO NP coated paper. (e) The embossment effect of the finger shown in (d). (f) A magnified image of the marked area in (e).

spectra of the $CuCl_2$ aqueous solution, the ZnO NP solution, and the mixed solution have been measured, as shown in Fig. S7 (ESI†). The absorption spectrum of the $CuCl_2$ solution matches little with the fluorescence spectrum of the ZnO NPs, indicating that the quenching cannot be caused by the absorbance of the ZnO NP fluorescence by the $CuCl_2$. Also, it is apparent in Fig. S7 (ESI†) that the absorption spectrum of the mixed solution coincides well with that of the ZnO NPs, indicating that the ZnO NPs have not been decomposed by the $CuCl_2$. To study whether electron transfer is responsible for the quenching, the bonding states of the $CuCl_2$ and ZnO NPs have been investigated using XPS, as shown in Fig. 3(b), note that the spectrum has been calibrated using that of C 1s (284.5 eV). The Cu $2p_{3/2}$ and Cu $2p_{1/2}$ peaks for the $CuCl_2$ are located at 935.6 eV and 955.6 eV, while those of the ZnO and $CuCl_2$ mixed sample shift to 934.9 eV and 954.9 eV, respectively. The shift to the lower energy side indicates that electrons have been partially transferred to the $CuCl_2$ in the mixed sample, and thus the fluorescence quenching of the ZnO NPs may be due to the transfer of electrons from the ZnO to the $CuCl_2$. To confirm this quenching mechanism, transient fluorescence spectroscopy at 525 nm has been measured for the mixed and pristine ZnO NP samples, as illustrated in Fig. 3(c). In Fig. 3(c), the scattered symbols are experimental data and the solid lines are the results of fitting the experimental data using the following two-order exponential decay formula:

$$y = y_0 + A_1 \exp(-t/\tau_1) + A_2 \exp(-t/\tau_2) \quad (1)$$

where y is the emission intensity, y_0, A_1, A_2 are constants, and t is time. The best fitting yields the lifetimes of τ_1 = 49.60 ns, and τ_2 = 1565.13 ns for pristine ZnO NPs, and τ_1 = 11.58 ns, and τ_2 = 162.24 ns for the mixed sample. The distinctively decreased carrier lifetime for the ZnO/$CuCl_2$ mixed sample compared with that of the pristine ZnO NPs verifies that some electrons have been transferred from the ZnO NPs to the $CuCl_2$ in the mixed sample. The electron transfer process has been illustrated schematically in the inset of Fig. 3(c).

Fingerprints have been considered to be unique identification of authorization with a relatively high security level. To demonstrate that the $CuCl_2$ quenched fluorescence of the ZnO NPs can be employed as fingerprint developer, a fingertip dipped into the $CuCl_2$ solution was pressed onto a piece of ZnO NP coated paper, and images of the fingerprints were captured with a digital camera under UV illumination, as shown in Fig. 3(d). The obtained fingerprint contours are clear, and the fingerprint has been transformed into an embossed image for more intuitive observation, as shown in Fig. 3(e) and (f).

3.3 The process of encryption and decryption

Using the fluorescence quenching characteristics of the ZnO NPs by both $CuCl_2$ and vinegar described above, an encryption process employing the ZnO NPs as the fluorescent reagent and $CuCl_2$ and vinegar as quenchers has been proposed, and this process is illustrated in Fig. 4.

Step 1, write-in. The ZnO NP solution was coated onto fluorescer-free paper, and the cartridge of an ink-jet printer was filled with $CuCl_2$ solution. Using the $CuCl_2$ solutions as ink, words were printed onto the ZnO NP coated paper. Under normal lighting conditions, the words are invisible, while under UV illumination the fluorescence of the ZnO NPs in the area with words has been quenched by the $CuCl_2$ while that in the other area remains, thus the words can be observed clearly.

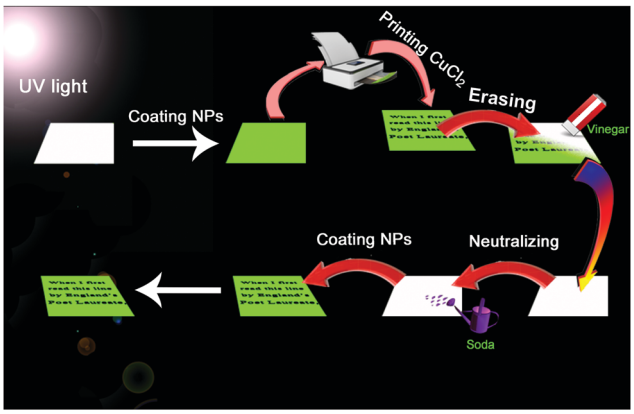

Fig. 4 The schematic illustration of the encryption and decryption process of words. The ZnO NPs were coated onto paper firstly, then words were printed onto the paper using $CuCl_2$ solution as ink, and vinegar vapour was used to erase the words. The paper was then neutralized with soda vapour, and finally recoating the ZnO NPs onto the paper decrypted the encrypted words.

Step 2, encryption. Put the paper with words for encryption in an ambient environment of vinegar vapour and the fluorescence of the ZnO NPs will be quenched by the vinegar, due to the decomposition of ZnO in acidic conditions. Thus the words will be invisible even under UV illumination, meaning that the words have been hidden and encrypted.

Step 3, decryption. Place the papers with encrypted words in an ambient environment of soda vapour to neutralize the absorbed vinegar, and then recoat ZnO NPs onto the whole paper. Thereafter, the ZnO NPs in the area without $CuCl_2$ will regain fluorescence under UV illumination, while the fluorescence is still quenched in the area with $CuCl_2$. Thus the encrypted words can be observed again.

3.4 Multiple grey levels printing test

For the encryption of complex patterns, images with multiple greyscale levels are needed. To test whether multiple grey levels can be realized when employing the ZnO NPs as the fluorescent reagent and $CuCl_2$ as the quencher, sixteen squares with different grey values have been printed onto ZnO NP pre-coated paper using $CuCl_2$ solution as ink, which was filled in the cartridge of an ink-jet printer, shown in Fig. 5(a). Each printed square has an obvious distinct optical density. For quantitative description, the sixteen squares have been transformed into a greyscale image using MATLAB to extract the corresponding grey values, as illustrated in Fig. 5(b). The grey level of each printed square is almost constant along the blue dashed line, while the grey value decreases as the compiled optical density increases, as revealed by the curve shown in the inset of Fig. 5(b). A logo image has been printed onto the ZnO NP pre-coated fluorescer-free paper *via* the same process, employing the $CuCl_2$ solution as

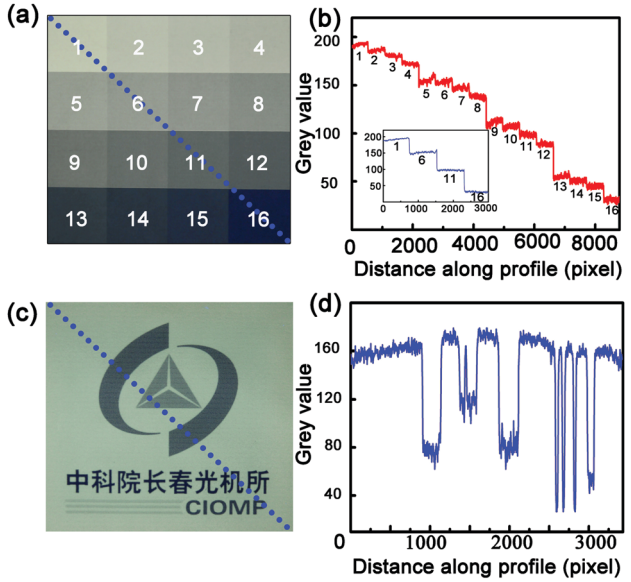

Fig. 5 (a) The printed squares with sixteen grey levels using $CuCl_2$ as ink on ZnO NP coated paper. (b) The variation of the grey value of every square. The inset shows the grey value along the blue dashed line in (a). (c) An image containing different grey values is printed using $CuCl_2$ as ink. (d) The variation of the grey value along the blue dashed line in (c).

ink, as shown in Fig. 5(c), and the grey values along the blue dashed line have been extracted, as indicated in Fig. 5(d). It is shown that the grey level along the dashed line can be depicted clearly, which reveals that complex patterns with multiple grey levels can be realized using the $CuCl_2$ ink on ZnO NP pre-coated paper.

3.5 Application for encryption

To demonstrate the decryption of complex patterns based on the strategy described above, an encoded portrait drawing (Mona Lisa by Leonardo Da Vinci) was printed onto a ZnO NP coated xerographic paper using $CuCl_2$ as ink. The image can be clearly observed under UV illumination, as indicated in Fig. 6(a). Then the paper was exposed to vinegar vapour, and the encrypted portrait disappears due to the fluorescence quenching caused by the decomposition of the ZnO in acidic conditions, as shown in Fig. 6(b). For decryption, after placing the paper in an ambient environment of soda vapour and then recoating ZnO NPs onto the whole paper uniformly, the image appears again, as indicated in Fig. 6(c). Furthermore, the grey value along the dashed line in Fig. 6(a)–(c) has been extracted to describe the image quality after these processes. The grey values along the highlighted dash lines in the image before and after decryption match well, as shown in Fig. 6(d), which indicates that the color quality of the image fades little after the encryption–decryption cycle.

To further enhance the anti-counterfeiting capability of this strategy, specific areas of the image (marked by the square at the angulus oris) have been encoded with a quadra-scaled matrix. A 4×4 matrix of discrete dots with given grey values is printed into the image as an additional tag, as shown in Fig. 6(e). Each dot has been transformed into pseudo-colour map with MATLAB for encoding, as presented in Fig. 6(f). The 4×4 matrix is divided into

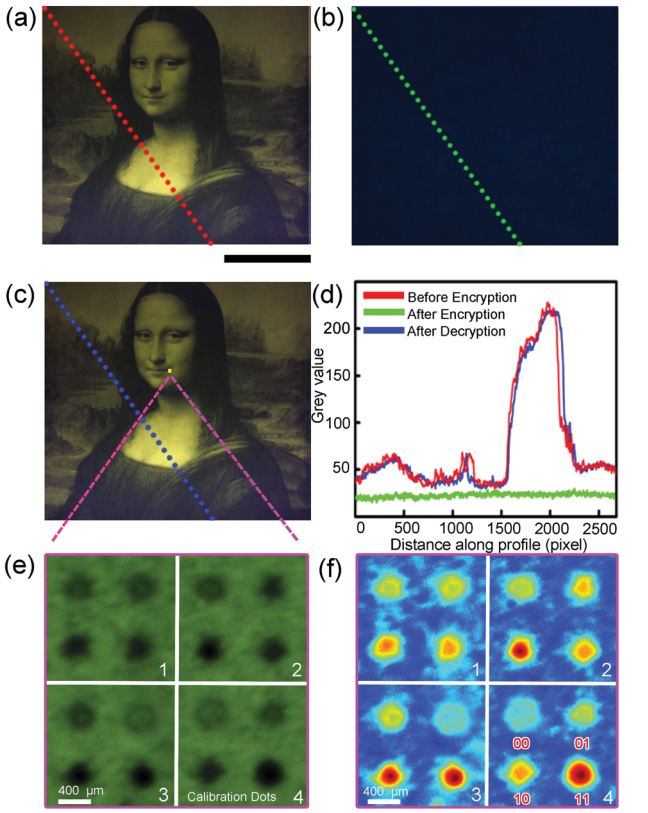

Fig. 6 (a) The image of Mona Lisa produced by printing $CuCl_2$ solution onto ZnO NP coated paper, and the scale bar is 7 cm. (b) The image was encrypted using vinegar. (c) The decrypted image after neutralizing and re-coating with ZnO NPs. (d) The grey values along the red, green, and blue dashed lines in (a), (b), and (c). (e) The 4×4 quadra-scaled matrixes for further encoding in the square marked in (c). (f) The pseudo-colour map of (e) produced with MATLAB.

four blocks labelled with 1, 2, 3, and 4. The former three blocks is for data encoding, in which each dot represents a specific bi-bit binary value, and the last dot is set as the standard for data calibration, in which the average grey value of each dot extracted has been set as "00", "01", "10" and "11". Therefore, from the dots in the upper left block, a series of codes "01", "01", "10", and "10" can be extracted, which represent the letter "Z" according to the binary American standard code for information interchange (ASCII) system. For the next two blocks, letters "n" and "O" can be extracted by the same process. The cryptogram "ZnO" could be then read out, which may be changed to any pre-designed characters, either in plaintext or in ciphertext. Then by varying the grey value of the 12 dots in the first three blocks while using that of the last block as a reference, a combination of a total of 412 ($= 1.67 \times 10^8$ codes) characters can be realized, which provides a huge hurdle for the counterfeiting of the encrypted information.

4 Conclusions

In summary, an advanced encryption strategy has been demonstrated based on the fluorescence quenching of ZnO by both

acid and $CuCl_2$. Using the $CuCl_2$ solutions as ink, words for encryption can be printed onto ZnO NP coated paper, and these are visible under UV illumination. The encryption is performed by simply exposing the paper to vinegar vapour, while the decryption is achieved by neutralization of the adsorbed vinegar with soda vapour and subsequent uniform re-coating with ZnO NPs. The encryption of grey scale images is also conducted by rendering complex patterns with $CuCl_2$ ink on the ZnO NP coated paper. To further enhance the anti-counterfeiting capability, a micron-sized matrix with a combination of a total of 1.67×10^8 codes is enciphered in a specific area of the image to be encrypted. The fluorescence quenching and regeneration process reported in this paper presents a promising strategy for advanced encryption, which may find wide applications in the fields of information security and anti-counterfeiting in the future.

Acknowledgements

This work is financially supported by the National Science Foundation for Distinguished Young Scholars of China (61425021), and the Natural Science Foundation of China (11374296, 51272238, 61376054, and U1604263).

Notes and references

1 M. Irie, T. Fukaminato, T. Sasaki, N. K. Tamai and T. Kawai, *Nature*, 2002, **420**, 759–760.
2 A. Kishimura, T. Yamashita, K. Yamaguchi and T. Aida, *Nat. Mater.*, 2005, **4**, 546–549.
3 K. Li, Y. Xiang, X. Wang, J. Li, R. Hu, A. Tong and B. Z. Tang, *J. Am. Chem. Soc.*, 2014, **136**, 1643–1649.
4 G.-S. Liou, S. H. Hsiao and T. H. Su, *J. Mater. Chem.*, 2005, **15**, 1812.
5 Y. Liu, K. R. Wang, D. S. Guo and B. P. Jiang, *Adv. Funct. Mater.*, 2009, **19**, 2230–2235.
6 T. Mutai, H. Satou and K. Araki, *Nat. Mater.*, 2005, **4**, 685–687.
7 Y. Sagara and T. Kato, *Nat. Chem.*, 2009, **1**, 605–610.
8 E. M. Lindh, A. Sandström, M. R. Andersson and L. Edman, *Light: Sci. Appl.*, 2016, **5**, e16050.
9 X. L. Lu and M. Xia, *J. Mater. Chem. C*, 2016, **4**, 9350–9358.
10 D. Qu, M. Zheng, J. Li, Z. Xie and Z. Sun, *Light: Sci. Appl.*, 2015, **4**, e364.
11 D. X. Ye, Y. Y. Ma, W. Zhao, H. M. Cao, J. L. Kong, H. M. Xiong and H. Mohwald, *ACS Nano*, 2016, **10**, 4294–4300.
12 K. Chang, Z. Liu, H. Chen, L. Sheng, S. X. Zhang, D. T. Chiu, S. Yin, C. Wu and W. Qin, *Small*, 2014, **10**, 4270–4275.
13 Z. Li, R. Liang, W. Liu, D. Yan and M. Wei, *Nanoscale*, 2015, **7**, 16737–16743.
14 K. Kumar, H. Duan, R. S. Hegde, S. C. Koh, J. N. Wei and J. K. Yang, *Nat. Nanotechnol.*, 2012, **7**, 557–561.
15 Y. Lu, J. Zhao, R. Zhang, Y. Liu, D. Liu, E. M. Goldys, X. Yang, P. Xi, A. Sunna, J. Lu, Y. Shi, R. C. Leif, Y. Huo, J. Shen, J. A. Piper, J. P. Robinson and D. Jin, *Nat. Photonics*, 2013, **8**, 32–36.
16 J. Andres, R. D. Hersch, J.-E. Moser and A.-S. Chauvin, *Adv. Funct. Mater.*, 2014, **24**, 5029–5036.
17 S. Han, H. J. Bae, J. Kim, S. Shin, S. E. Choi, S. H. Lee, S. Kwon and W. Park, *Adv. Mater.*, 2012, **24**, 5924–5929.
18 B. Yoon, J. Lee, I. S. Park, S. Jeon, J. Lee and J.-M. Kim, *J. Mater. Chem. C*, 2013, **1**, 2388.
19 X. Xie, Z. Li, Y. Zhang, S. Guo, A. I. Pendharkar, M. Lu, L. Huang, W. Huang and G. Han, *Small*, 2017, **13**, 1602843.
20 L. Shi, Y. Li, X. Li, X. Wen, G. Zhang, J. Yang, C. Dong and S. Shuang, *Nanoscale*, 2015, **7**, 7394–7401.
21 X. Sun, K. Yin, B. Liu, S. Zhou, J. Cao, G. Zhang and H. Li, *J. Mater. Chem. C*, 2017, **5**, 4951–4958.
22 B. Bao, M. Li, Y. Li, J. Jiang, Z. Gu, X. Zhang, L. Jiang and Y. Song, *Small*, 2015, **11**, 1649–1654.
23 X. Chen, Q. Jin, L. Wu, C. Tung and X. Tang, *Angew. Chem., Int. Ed.*, 2014, **53**, 12542–12547.
24 J. Zhang, Y. Yuan, G. Liang, M. N. Arshad, H. A. Albar, T. R. Sobahi and S. H. Yu, *Chem. Commun.*, 2015, **51**, 10539–10542.
25 R. Klajn, P. J. Wesson, K. J. Bishop and B. A. Grzybowski, *Angew. Chem., Int. Ed.*, 2009, **48**, 7035–7039.
26 S. Qu, X. Wang, Q. Lu, X. Liu and L. Wang, *Angew. Chem., Int. Ed.*, 2012, **51**, 12215–12218.
27 M. Gu, X. Li and Y. Cao, *Light: Sci. Appl.*, 2014, **3**, e177.
28 S. Zhu, Q. Meng, L. Wang, J. Zhang, Y. Song, H. Jin, K. Zhang, H. Sun, H. Wang and B. Yang, *Angew. Chem., Int. Ed.*, 2013, **52**, 3953–3957.
29 Q. Lou, S. Qu, P. Jing, W. Ji, D. Li, J. Cao, H. Zhang, L. Liu, J. Zhao and D. Shen, *Adv. Mater.*, 2015, **27**, 1389–1394.
30 X. Hou, C. Ke, C. J. Bruns, P. R. McGonigal, R. B. Pettman and J. F. Stoddart, *Nat. Commun.*, 2015, **6**, 6884.
31 Bruce Hardwick, Wayne Jackson, Gerard Wilson and A. W. H. Mau, *Adv. Mater.*, 2001, **13**, 12–13.
32 C. Huang, B. Lucas, C. Vervaet, K. Braeckmans, S. Van Calenbergh, I. Karalic, M. Vandewoestyne, D. Deforce, J. Demeester and S. C. De Smedt, *Adv. Mater.*, 2010, **22**, 2657–2662.
33 E. L. Prime and D. H. Solomon, *Angew. Chem., Int. Ed.*, 2010, **49**, 3726–3736.
34 A. Mullard, *Nat. Med.*, 2010, **16**, 361.
35 H. Sun, S. Liu, W. Lin, K. Y. Zhang, W. Lv, X. Huang, F. Huo, H. Yang, G. Jenkins, Q. Zhao and W. Huang, *Nat. Commun.*, 2014, **5**, 3601.
36 H. M. Xiong, *Adv. Mater.*, 2013, **25**, 5329–5335.
37 K. Matsuyama, N. Ihsan, K. Irie, K. Mishima, T. Okuyama and H. Muto, *J. Colloid Interface Sci.*, 2013, **399**, 19–25.
38 Z. Y. Zhang, Y. D. Xu, Y. Y. Ma, L. L. Qiu, Y. Wang, J. L. Kong and H. M. Xiong, *Angew. Chem., Int. Ed.*, 2013, **52**, 4127–4131.
39 X. Cai, Y. Luo, W. Zhang, D. Du and Y. Lin, *ACS Appl. Mater. Interfaces*, 2016, **8**, 22442–22450.
40 N. Tripathy, R. Ahmad, H. A. Ko, G. Khang and Y.-B. Hahn, *Nanoscale*, 2015, **7**, 4088–4096.
41 R. Zhou, Q. Zhao, K.-K. Liu, Y.-J. Lu, L. Dong and C.-X. Shan, *J. Mater. Chem. C*, 2017, **5**, 1685–1691.

42 N. Park, K. Sun, Z. Sun, Y. Jing and D. Wang, *J. Mater. Chem. C*, 2013, **1**, 7333.
43 Y. J. Lu, Z. F. Shi, C. X. Shan and D. Z. Shen, *Chin. Phys. B*, 2017, **26**, 047703.
44 P. K. Shrestha, Y. T. Chun and D. Chu, *Light: Sci. Appl.*, 2015, **4**, e259.
45 W. Ji, T. Wang, B. Zhu, H. Zhang, R. Wang, D. Zhang, L. Chen, Q. Yang and H. Zhang, *J. Mater. Chem. C*, 2017, **5**, 4543–4548.
46 Z. F. Shi, Y. Li, Y. T. Zhang, Y. S. Chen, X. J. Li, D. Wu, T. T. Xu, C. X. Shan and G. T. Du, *Nano Lett.*, 2017, **17**, 313–321.
47 J. Pan, J. Chen, Q. Huang, Q. Khan, X. Liu, Z. Tao, Z. Zhang, W. Lei and A. Nathan, *ACS Photonics*, 2016, **3**, 215–222.
48 C. Lu, X. Hu, K. Shi, Q. Hu, R. Zhu, H. Yang and Q. Gong, *Light: Sci. Appl.*, 2015, **4**, e302.
49 C. Liu, Z. Liu, J. Li, Y. Li, J. Han, Y. Wang, Z. Liu and J. Ya, *Microelectron. Eng.*, 2013, **103**, 12–16.
50 Y. J. Shin, K. S. Kim, N. G. Park, K. S. Ryu and S. H. Chang, *Bull. Korean Chem. Soc.*, 2005, **26**, 1929–1930.
51 A. Sadollahkhani, A. Hatamie, O. Nur, M. Willander, B. Zargar and I. Kazeminezhad, *ACS Appl. Mater. Interfaces*, 2014, **6**, 17694–17701.
52 Z. Chen and D. Wu, *Sens. Actuators, B*, 2014, **192**, 83–91.
53 S. M. Ng, D. S. Wong, J. H. Phung, S. F. Chin and H. S. Chua, *Talanta*, 2013, **116**, 514–519.
54 K. K. Liu, C. X. Shan, H. Z. Liu, Q. Lou and D. Z. Shen, *RSC Adv.*, 2017, **7**, 1841–1846.
55 K. K. Liu, C. X. Shan, G. H. He, R. Q. Wang, L. Dong and D. Z. Shen, *Sci. Rep.*, 2017, **7**, 42232.
56 S. Monticone, R. Tufeu and A. V. Kanaev, *J. Phys. Chem. B*, 1998, **102**, 2854–2862.
57 X. Wang, X. G. Kong, Y. Yu and H. Zhang, *J. Phys. Chem. C*, 2007, **111**, 3836–3841.
58 A. Asok, M. N. Gandhi and A. R. Kulkarni, *Nanoscale*, 2012, **4**, 4943–4946.
59 S. W. Bian, I. A. Mudunkotuwa, T. Rupasinghe and V. H. Grassian, *Langmuir*, 2011, **27**, 6059–6068.